Ultrafine particles in four European urban environments: results from a new continuous long-term monitoring network

J. Hofman[1]*, J. Staelens[1], R. Cordell[2], C. Stroobants[1], N. Zikova[3], S.M.L. Hama[2,4], K.P. Wyche[5], G.P.A. Kos[6], S. Van Der Zee[7], K.L. Smallbone[5], E.P. Weijers[6], P.S. Monks[2], E. Roekens[1]

[1]*Flanders Environment Agency (VMM), Department Air, Environment and Communication, Belgium*
[2]*University of Leicester, Department of Chemistry, United Kingdom*
[3]*Institute for Environmental Studies, Faculty of Science, Charles University, Prague, Czech Republic*
[4]*Department of Chemistry, School of Science, University of Sulaimani, Kurdistan Region, Sulaimani, Iraq*
[5]*Air Environment Research, University of Brighton, School of Environment and Technology, United Kingdom*
[6]*Energy research Centre of the Netherlands (ECN), Environment & Energy Engineering, the Netherlands*
[7]*Public Health Service of Amsterdam, Department of Air Quality, the Netherlands*

Current affiliation corresponding author:
Research Foundation Flanders (FWO)
University of Antwerp
Department of Bioscience Engineering
Groenenborgerlaan 171
2020 Antwerp
Belgium

Abstract

To gain a better understanding on the spatiotemporal variation of ultrafine particles (UFPs) in urban environments, this study reports on the first results of a long-term UFP monitoring network, set up in Amsterdam (NL), Antwerp (BE), Leicester (UK) and London (UK). Total number concentrations and size distributions were assessed during 1-2 years at four urban background sites, supplemented with a mobile trailer for co-location monitoring and additional short-term sites. Intra- and interurban spatiotemporal UFP variation, associations with commonly-monitored pollutants (PM, NO_x and BC) and impacts of wind fields were evaluated. Although comparable size distributions were observed between the four cities, source-related differences were demonstrated within specific particle size classes. Total and size-resolved particle number concentrations showed clear traffic-related temporal variation, confirming road traffic as the major UFP contributor in urban environments. New particle formation events were observed in all cities. Correlations with typical traffic-related pollutants (BC and NO_x) were obtained for all monitoring stations, except for Amsterdam, which might be attributable to UFP emissions from Schiphol airport emissions. The temporal variation in particle number concentration correlated fairly weakly between the four cities (r_s = 0.28-0.50, COD = 0.28-0.37), yet improved significantly inside individual cities (r_s = 0.59-0.77). Nevertheless, considerable differences were still obtained in terms of particle numbers (20-38% for total particle numbers and up to 49% for size-resolved particle numbers), confirming the importance of local source contributions and the need for careful consideration when allocating UFP monitoring stations in heterogeneous urban environments.

1. Introduction

Atmospheric aerosols, ranging from several nanometers to approximately 100 micrometers in diameter, are composed of primary particles, emitted from both anthropogenic activities and natural sources, and secondary particles formed by gas-to-particle conversion processes including nucleation

46 and condensation (Donaldson et al., 2001; Querol et al., 2011; Viana et al., 2015). They are typically
47 characterized by varying size modes, i.e. <10 nm (nucleation), 10-100 nm (Aitkin mode), 100 nm - 1 µm
48 (accumulation mode) and coarse mode (>1 µm), providing information on the contributing emission
49 sources and attributing chemical and physical processes (Vu et al., 2015). Current air quality legislation
50 focusses on monitoring, limiting and reducing mass concentrations of these airborne particles.
51 However, recent toxicological and epidemiological research suggests that particle numbers may
52 constitute better links to health endpoints than mass concentration (Donaldson et al., 2001; Harrison
53 et al., 2000; Kelly and Fussell, 2012). Ultrafine particles (UFPs) in particular, consisting of aerosols
54 smaller than 100 nm, have been demonstrated to cause adverse health effects owing to their ability
55 to penetrate deeply into the respiratory system and enter the bloodstream inducing inflammation and,
56 potentially promoting cardiovascular and respiratory conditions. In ambient air, ultrafine particles are
57 dominant in terms of particle number (80-90% of all particles), but negligible in terms of particle mass,
58 and are, therefore, inadequately quantified in current (mass-based) air quality monitoring networks.
59 This especially holds true in urban areas, where concentrated local emissions sources and a complex
60 urban topography are known to reduce pollutant dispersion. Consequently, there is a clear need for a
61 thorough understanding of the spatiotemporal variation of UFPs.

62 There have been several short-term studies which have contributed to existing knowledge on the
63 number/size distribution of specific UFP sources, and attributing formation and transformation
64 processes of UFPs (Brines et al., 2015; Dall'Osto et al., 2013; González et al., 2011; Hudda et al., 2014;
65 Keuken et al., 2015; Kozawa et al., 2012; Zhu et al., 2002). Studies reporting on long-term simultaneous
66 UFP measurements at multiple sites are, however, scarce (Pey et al., 2008; Reche et al., 2011; von
67 Bismarck-Osten et al., 2013). Nevertheless, such networks are vital to elucidate the complex
68 relationship between local emission sources, meteorological processes, atmospheric transformation
69 and the resulting aerosol number, size and distribution at sites with differing characteristics. This study
70 reports on the first results of a novel North-West European UFP monitoring network, established in
71 Amsterdam, Antwerp, Leicester and London. The work was carried out as part of the Joint Air Quality
72 Initiative (www.joaquin.eu), an INTERREG IVB funded European project, aimed at supporting health-
73 oriented air quality policies in Europe. The main aims were to gain more insight in the spatiotemporal
74 variation in UFP number concentration and size distribution and to assess the added value of UFP data
75 compared to more commonly measured parameters such as particulate matter (PM_x) and nitrogen
76 oxides (NO_x).

77 **2.   Material and methods**
78 2.1 Monitoring sites

79 An UFP monitoring network was set up in four NW European cities (*Figure 1*), consisting of four fixed
80 monitoring sites at urban background locations in Amsterdam (the Netherlands; AD1), Antwerp
81 (Belgium; AP1), Leicester (United Kingdom; LE1) and London (United Kingdom; LO1). In addition to the
82 fixed monitoring sites, a mobile monitoring unit was deployed for comparative UFP measurements
83 collocated with all fixed monitoring sites (1M) and for additional UFP measurements at a second urban
84 background site (2M) in Amsterdam (6.2 km from AD1), Antwerp (1.3 km from AP1) and Leicester (1.2
85 km from LE1). Hence, UFPs were measured at seven urban background locations across NW Europe
86 (*Figure 1*).

87 The UFP measurements started in April 2013 in Amsterdam and Antwerp, and later in Leicester
88 (November 2013) and London (April 2014) owing to legislation issues. Results up to March, 2015, are

89　discussed, hence the discussion covers a period of 1 to 2 years depending on the site considered. The
90　measurements by the mobile monitoring unit were carried out during 2-4 weeks next to the fixed
91　stations and during 2-7 weeks at the additional urban background sites (AD2M, AP2M, LE2M) (Table
92　1).

93 *Table 1: Overview of the applied fixed and mobile unit monitoring sites of the UFP monitoring network*

City	Code	Fixed/Mobile	Name	Distance to main street (m)	Traffic intensity* (veh/day)	Coordinates		Monitoring period	
						Latitude	Longitude	Start	End
Amsterdam	AD1	Fixed	Vondelpark	64	15000	52°21'35" N	4°51'59" E	01/04/2013	31/03/2015
	AD1M	Mobile	Vondelpark	64	15000	52°21'35" N	4°51'59" E	17/04/2013	14/05/2013
	AD2M	Mobile	Nieuwendammerdijk	20	<500	52°23'21" N	4°56'38" E	14/05/2013	30/05/2013
Antwerp	AP1	Fixed	Borgerhout	30	29500	51°12'35" N	4°25'55" E	01/04/2013	31/03/2015
	AP1M	Mobile	Borgerhout	30	29500	51°12'35" N	4°25'55" E	04/11/2013	19/11/2013
	AP2M	Mobile	Stadspark	45	7800	51'12'48" N	4°24'51" E	07/10/2013	04/11/2013
Leicester	LE1	Fixed	Leicester University	140	22500	52°37'12" N	1°07'38" E	25/10/2013	31/03/2015
	LE1M	Mobile	Leicester University	140	22500	52°37'12" N	1°07'38" E	04/03/2014	04/04/2014
	LE2M	Mobile	Brookfield	150	20500	52°37'15" N	1°06'32" E	05/04/2014	29/05/2014
London	LO1	Fixed	Eltham	60	16500	51°27'09" N	0°04'14" E	21/04/2014	31/03/2015
	LO1M	Mobile	Eltham	60	16500	51°27'09" N	0°04'14" E	02/06/2014	30/06/2014

94 *Mean traffic intensity (vehicles/day) at the nearest main street

95

96
97
98 *Figure 1: Overview of the UFP monitoring network: four fixed urban background sites in Amsterdam (AD1; NL), Antwerp (AP1; BE), Leicester (LE1; UK) and London (LO1; UK)*
99 *and the mobile monitoring unit for additional UFP measurements at a second urban background site in three cities (AD2M, AP2M and LE2M).*

100   2.2 Instrumentation

101   2.2.1   Air quality data

102   Several commercially available UFP instruments were evaluated via a comprehensive literature review
103   and laboratory test, in order to choose the most appropriate instrumentation and methodology for
104   particle number and size distribution measurements under continuous monitoring network conditions.
105   Based on this evaluation, three instruments were selected for application in the UFP monitoring
106   network (*Table 2*).

107   *Table 2: Specifications of the employed UFP instrumentation*
108

Name	Company/type	Lower size (nm)	Upper size (nm)	UFP size classes	Sample time (min)	Radioactive source	Condesation fluid	Deployed sites
EPC	TSI 3783	7	1000	1	1	-	Water	All
UFPM	TSI 3031	20	500	6	10	-	-	LE1, LO1 and Mobile
SMPS	Grimm 5420+CL-DMA	10	1000	45	10	^{85}Kr (185 Mbq)	Butanol	AD1, AP1 and Mobile

109

110   Total UFP number concentrations (TNC; # cm^{-3}) were obtained by means of a water-based
111   Environmental Particle Counter (EPC) at each monitoring station. After initial tests, the high-flow inlet
112   mode (3 l min^{-1}) was applied to minimize particle losses. Size-resolved particle number concentrations
113   (PNC; # cm^{-3}) were obtained using two different instruments (UFPM and SMPS) owing to legislation
114   issues with the radioactive source (^{85}Kr) at the UK sites. In Amsterdam (AD1) and Antwerp (AP1),
115   particle number concentrations in 45 different size classes were obtained by a scanning mobility
116   particle sizer (SMPS). In Leicester (LE1) and London (LO1), UFPs were quantified in six size classes (20-
117   30, 30-50, 50-70, 70-100, 100-200 and >200 nm), using an UFPM (Table 2). In brief, the operating
118   principle of the SMPS comprises radioactive (^{85}Kr) charging of particles, followed by size segregation
119   based on particle electrical mobility using a differential mobility analyser (L-DMA) and particle counting
120   by means of a butanol-based condensation particle counter (CPC). The UFPM principle of operation is
121   based on electrical diffusion charging of the particles, size segregation by means of a DMA, followed
122   by aerosol detection using a Faraday cup electrometer.

123

124   A Multi-Angle Absorption Photometer (MAAP 5021, Thermo Scientific) was installed in all monitoring
125   stations to determine ambient black carbon (BC) concentrations (μg m^{-3}), using the default specific
126   attenuation factor (sigma) of 6.6 m^2 g^{-1}, based on Petzold et al. (2002). In addition to the UFP and BC
127   instruments in the fixed monitoring stations, continuous air quality monitors were already available
128   for NO$_x$ (Thermo 42i in AP1, LE1 and LO1 and a API 200A in AD1), PM$_{10}$ (BAM1020 in AD1, ESM FH62 I-
129   R and FIDAS 200 in AP1 and TEOM-FDMS in LO1) and PM$_{2.5}$ (BAM1020 in AD1, ESM FH62 I-R and FIDAS
130   200 in AP1 and TEOM-FDMS in LE1 and LO1). The mobile monitoring unit was equipped with all UFP
131   instrumentation (EPC, UFPM, SMPS) and a MAAP 5012 for atmospheric BC measurements. For the EPC
132   and UFPM instruments an Environmental Sampling System (ESS; TSI 3031200) was used with a PM$_{10}$
133   inlet, sharp-cut PM$_1$ cyclone and Nafion dryer. The EPC in AD1 and AP1 were individually connected to
134   an ESS. In LE1, LO1 and the trailer, two instruments (EPC and UFPM) were connected to one ESS. The
135   SMPS devices had an individual Grimm sampling system with TSP inlet and Nafion dryer. Standard
136   operating procedures were created for the applied instrumentation to ensure that comparable
137   monitoring data was collected at the seven locations (monitoring artefacts, e.g. inlet systems,
138   maintenance frequency etc.).

139 Before the instruments were installed at the monitoring sites, they were intercompared in an initial
140 co-location monitoring campaign from December 2012 to January 2013 at an urban background
141 location in Antwerp (Frijns et al., 2013). All EPCs and SMPSs were strongly correlated and differed by
142 less than 10% (except for the LE1 EPC; 13%, probably due to the sampling setup which was changed
143 following the colocation trial). The total number concentration, quantified by the EPC, was
144 approximately 20% higher compared to the SMPS and 24% higher compared to the UFPM. More details
145 on the instrument comparisons can be found in the report by (Frijns et al., 2013). After installing the
146 instruments at their monitoring locations, the mobile monitoring unit performed measurements
147 adjacent to each monitoring site to evaluate the agreement of the instruments and reliability of the
148 conducted measurements. Results of the mobile monitoring unit comparison can be found in the final
149 Joaquin reporting (Joaquin, 2015).

2.2.2 Meteorological data

151 Meteorological data of ambient air temperature (°C), relative humidity (%), atmospheric pressure (Pa),
152 wind direction (°) and speed (m s^{-1}) were obtained for each monitoring site. Meteorological parameters
153 (e.g. wind) can be altered significantly at the local scale due to the urban canopy (e.g. building height,
154 street orientation etc). Therefore, regional meteorological data were collected in addition to enable
155 evaluation of larger-scale air mass transport processes. Regional meteorology was measured at a
156 distance of 9 km from AD1 (Schiphol airport), 6 km from AP1 (Luchtbal monitoring station of the
157 Flanders Environment Agency, VMM), 5 km from LE1 (Groby Road monitoring station) and 14 km from
158 LO1 (Barking and Dagenham – Rush Green monitoring station).

2.3 Data validation and treatment

160 The raw 10 minute-data were validated by screening for irregularities and removing data collected
161 during instrument errors and maintenance periods. All validated data were subsequently aggregated
162 to 30 minute intervals. The retain threshold in further data averaging was 75% availability at the half-
163 hourly level. For comparison purposes between the considered monitoring sites, size-resolved UFP
164 concentrations, obtained by the SMPS (45 size classes), were aggregated to the UFPM size classes: 10-
165 20, 20-30, 30-50, 50-70, 70-100 and 100-200 nm.

166 Boxplots, single linear regression plots, coefficients of divergence (COD) and Spearman Rank (r$_s$)
167 correlations were applied to compare monitoring sites, time periods and pollutants. The COD provides
168 information on the degree of uniformity between monitoring stations and is defined as

169
$$COD_{xy} = \sqrt{\frac{1}{n}\sum_{i=1}^{n}\left(\frac{c_{ix}-c_{iy}}{c_{ix}+c_{iy}}\right)^2}$$

170 where x and y are the different monitoring stations, c_{ix} is the ith observation of the pollutant
171 concentration at monitoring location x, and n is the number of observations. Small COD values imply
172 similarities between the concentrations measured at various sites, while COD values approaching unity
173 indicate vast differences between sites.

174 Potential effects of wind speed and direction were evaluated using pollution roses and polar plots. All
175 statistical analyses were performed using the statistical software package R (R Development Core
176 Team, 2015), more specifically in the *openair* package (Carslaw and Ropkins, 2015, 2012).

3. Results and Discussion

3.1 Data exploration

The 30 minute air quality and meteorological data were collected for the entire sampling period, from April, 2013, to March, 2015. Taking into account the later start of the UFP measurements in Leicester and London (Table 1), data coverage at the 30 minute was 96% for BC, 79% for total particle number concentrations (TNC) and 83% for size-resolved particle number concentrations (PNC). This is comparable but generally lower than for the more commonly monitored pollutants NO_2 (89%), PM_{10} (94%) and $PM_{2.5}$ (81%). The data range of PM, NO_2, BC and TNC was fairly comparable across the considered monitoring locations, except for Antwerp where higher overall concentrations of the typical traffic-related pollutants (NO_x, BC and TNC) were observed (Table 3). This can be explained by its proximity (30 m) to a traffic-intensive access road into Antwerp (*Plantin en Moretuslei*). In February and October 2013, the mean traffic volume was 32000 vehicles on weekdays and 23500 vehicles in the weekend; or a time-weighted average of 29500 vehicles/day (VMM, 2014).

Looking at the range of the quantified total and size-resolved PNC (*Table 3*), comparable UFP variability was found at the monitoring sites, with the highest PNC observed in Antwerp. For all monitoring sites, the highest PNC were obtained in the smallest particle size class (10-20 nm), consecutively followed by the 30-50, 20-30, 50-70, 70-100 and 100-200 nm size classes. In Leicester and London, the 10-20 nm size class was not quantified due to the size range restrictions of the applied UFPM (see *Table 2*). Nevertheless, comparable behaviour of the 10-20 nm size class was observed from co-located SMPS measurements during the 2-4 week instrument comparison conducted by the co-located mobile monitoring unit (Joaquin, 2015).

	Amsterdam (AD1)	Antwerp (AP1)	Leicester (LE1)	London (LO1)		Amsterdam (AD1)	Antwerp (AP1)	Leicester (LE1)	London (LO1)
PM_{10} ($\mu g\ m^{-3}$)					PNC 10-20 nm (# cm^{-3})				
25% quartile	12.24	15.00	-	11.30	25% quartile	1125	1327	-	-
mean	20.64	25.99	-	18.64	mean	2592	2468	-	-
75% quartile	25.21	32.50	-	22.50	75% quartile	2956	3093	-	-
max	227.50	176.25	-	122.50	max	56575	35412	-	-
$PM_{2.5}$ ($\mu g\ m^{-3}$)					PNC 20-30 nm (# cm-3)				
25% quartile	6.82	7.00	6.70	6.10	25% quartile	805	974	755	475
mean	14.24	16.17	13.47	13.00	mean	1552	1709	1541	1007
75% quartile	17.66	20.47	16.70	15.90	75% quartile	1773	2112	2001	1191
max	225.30	145.00	181.00	90.40	max	39199	19634	13795	29072
NO_2 ($\mu g\ m^{-3}$)					PNC 30-50 nm (# cm-3)				
25% quartile	14.00	24.00	14.20	9.20	25% quartile	1031	1278	891	811
mean	25.49	41.37	27.13	20.63	mean	1773	2195	1774	1539
75% quartile	34.00	55.00	36.20	28.60	75% quartile	2163	2704	2227	1946
max	107.00	242.00	117.80	105.70	max	19756	26669	16641	22534
NO ($\mu g\ m^{-3}$)					PNC 50-70 nm (# cm-3)				
25% quartile	0.40	2.00	1.80	1.30	25% quartile	537	717	594	426
mean	4.89	17.56	11.07	6.60	mean	950	1267	1247	809
75% quartile	4.00	18.00	10.60	4.90	75% quartile	1215	1598	1539	1042
max	230.03	784.00	540.00	321.10	max	8907	15387	14614	8959
BC ($\mu g\ m^{-3}$)					PNC 70-100 nm (# cm-3)				
25% quartile	0.49	1.11	0.61	0.52	25% quartile	362	553	504	400
mean	1.01	2.36	1.40	1.22	mean	759	1063	1112	776
75% quartile	1.29	3.00	1.70	1.49	75% quartile	1026	1382	1363	1012
max	9.56	19.52	16.05	12.13	max	5546	5765	17444	10074
TNC (# cm^{-3})					PNC 100-200 nm (# cm-3)				
25% quartile	5889	8713	4760	5230	25% quartile	363	604	447	319
mean	9070	13481	8623	8353	mean	807	1182	1010	711
75% quartile	10952	16538	10916	10506	75% quartile	1069	1531	1233	936
max	76549	76170	63481	45155	max	20116	11903	19702	12707

200

201   3.2 Temporal variation in TNC

202   From the temporal variation plots of hourly-, daily- and monthly-averaged TNC, higher TNC are clearly
203   observed in Antwerp, when compared to Amsterdam, Leicester and London (Figure 2). A typical traffic-
204   related diurnal variation was observed throughout the day, with distinct morning and evening peaks
205   coinciding with traffic rush hours. During the weekends, the peaks were less pronounced and negligible
206   during the morning rush hour, which seems to confirm road traffic as the main UFP attributor in urban
207   environments, as reported earlier (Goel and Kumar, 2015; Kumar et al., 2014; Mishra et al., 2012;
208   Querol et al., 2011; Reche et al., 2011). This was further confirmed when examining the temporal
209   variation of BC (Appendix 1), which can be considered as a typical traffic-related pollutant. Similar
210   diurnal variations, with distinct morning and evening peaks, and decreased concentrations during the
211   weekend were identified. For all monitoring sites, the highest monthly-averaged TNC were obtained
212   during winter months (September-March). This is likely due to meteorological conditions (e.g.
213   temperature and mixing layer height) favouring higher atmospheric UFP concentrations, as reported
214   before by Mishra et al. (2012), Pey et al. (2008) and von Bismarck-Osten et al. (2013).

215
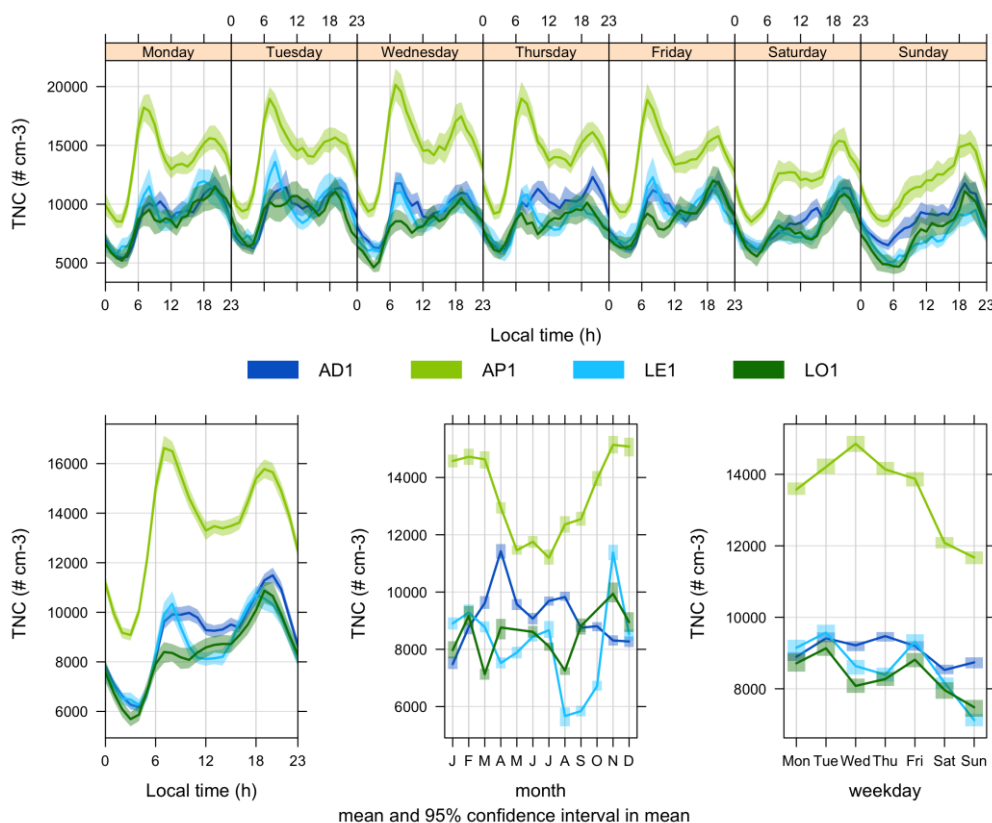
Figure 2: Temporal variation of total particle number concentration (TNC; # cm^{-3}) at the four fixed monitoring
sites (AD1, AP1, LE1 and LO1) at three different time scales (hourly, daily and monthly averages). The coloured
zone represents the 95% confidence interval.

219   For the hourly-averaged diurnal UFP variation per particle size class (*Figure 3*), comparable findings as
220   for the TNC were observed, with a more or less constant ratio of the individual size classes, indicating
221   a fairly stable UFP size distribution throughout time (also observed for the daily- and monthly-averaged
222   PNC). However, temporal differences were observed for the 10-20 nm particle size class, which was

223 only quantified in Amsterdam and Antwerp. For Amsterdam, a much higher relative contribution of
224 the 10-20 nm class with respect to the other particle size classes was found compared to Antwerp
225 (*Figure 3*). Moreover, a constant contribution (>3000 particles cm^{-3}) was observed throughout the day
226 (7:00-20:00h), while in Antwerp, the 10-20 nm sized particles followed the morning and evening rush
227 hour peaks (Appendix 2). Also during the weekends, an average constant contribution of 10-20 nm
228 sized particles was observed, while the PNC of all other size classes are observed to decrease
229 considerably (Appendix 2). These data, therefore, suggest a non-traffic related input of mainly smaller-
230 sized particles in Amsterdam. This UFP source seems to persist throughout the weekend, with the 10-
231 20 nm size channel exhibiting a diurnal variation that is comparable to that observed during the
232 working week. There was no clear decrease in the average PNC during the weekends, nor was there a
233 seasonal influence.
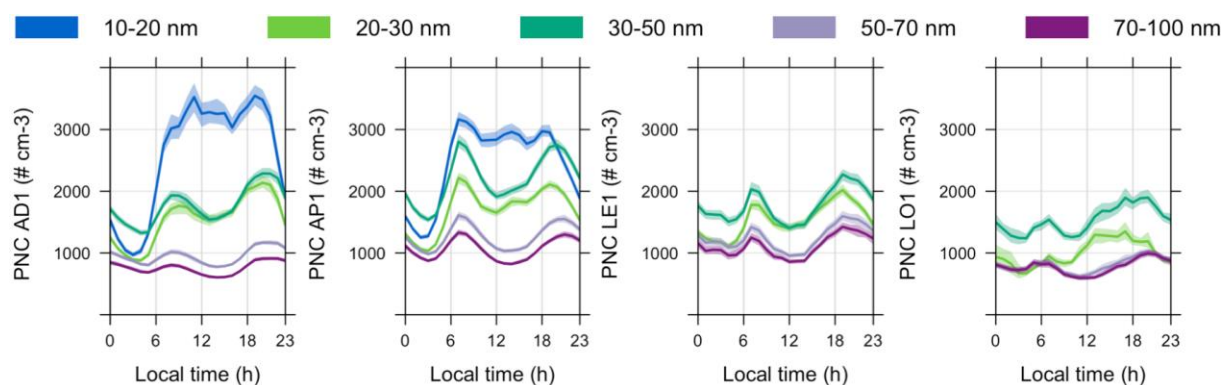
234

235 *Figure 3: Temporal variation of the hourly-averaged particle number concentration (PNC; # cm^{-3}) within the*
236 *individual UFP size classes (10-20 nm, 20-30 nm, 30-50 nm, 50-70 nm, 70-100 nm) at the four fixed monitoring*
237 *sites (AD1, AP1, LE1 and LO1).*
238

239   3.3 New particle formation events

240 In Antwerp, the hourly-averaged 10-20 nm sized particles exhibit a distinct small midday-peak (Figure
241 3), which was not observed for the other particle size classes (only to a limited extent in the 20-30 nm
242 size class). This observation resembles at new photochemical particle formation (NPF) events in urban
243 areas, as described in former studies (Brines et al., 2015; Kulmala and Kerminen, 2008; Pey et al., 2008;
244 Querol et al., 2011; Reche et al., 2011; Wang et al., 2014).

245 Plotting the half-hourly averaged SMPS data (45 size bins) of the fixed urban locations, multiple days
246 containing new particle formation (NPF) events could be identified in each city. While detailed size-
247 resolved particle number concentrations could be collected from the SMPS measurements in
248 Amsterdam (AD1; 730 days) and Antwerp (AP1; 730 days), only 6 UFP size classes were quantified by
249 the UFPM in Leicester (LE1) and London (LO1). We, therefore, collected SMPS data from the co-located
250 mobile unit to evaluate NPF events in Leicester (LE1M; 31 days) and London (LO1M; 28 days). Although
251 the monitoring period was much shorter in Leicester and London, distinct nucleation events were
252 observed at all monitoring locations, with 10-20 nm particle bursts starting around noon (N) and lasting
253 for approximately 2-4 hours during which a modest growth in particle diameter can be observed of up
254 to 40 nm (G), eventually suppressed by the condensation sink of the evening rush hour (Figure 4). Road
255 traffic emissions (T) can be observed, solely during evening rush hours on weekend days or holidays
256 (AD1, AP1, LE and LO), while morning rush hours are also observed on working days (AD2 and AP2).
257 While road traffic emissions (T) are clearly in the 30-50 nm size range, newly formed particles are much

258 smaller, namely (<) 10 nm which is the detection limit of the SMPS. The condensation sink effect of
259 local traffic emissions, restraining growth of nucleation mode particles (Brines et al., 2015), can clearly
260 be observed when comparing nucleation events between weekend/holidays and working days (AD$_1$ vs
261 AD$_2$ and AP$_1$ vs AP$_2$ in Figure 4).

262
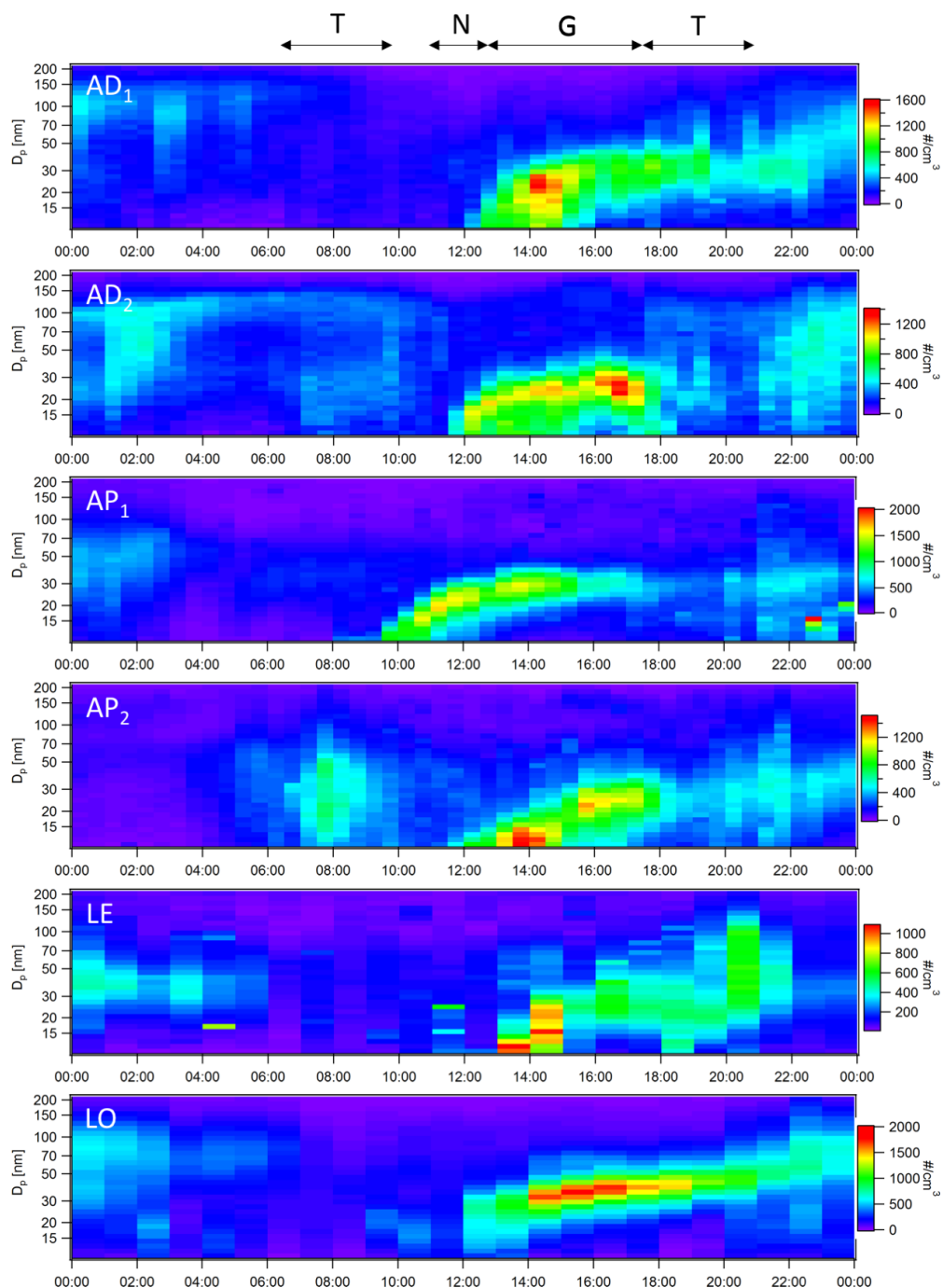
Figure 4: Size-resolved (nm) particle number concentration maps (# cm^{-3}) based on half-hourly averaged SMPS data during days with new particle formation (NPF) events in Amsterdam (AD1; 17/5/2014 and AD2; 17/6/2013), Antwerp (AP1; 9/5/2013 (Ascension day) and AP2; 16/9/2013), Leicester (LE; 16/3/2014) and London (LO; 8/6/2014). Nucleation events are characterised by a nucleation burst phase (N), followed by a particle growth phase (G).

268 Following the classification procedure of Dal Maso et al. (2005), the considered monitoring days were
269 classified as *event* or *non-event* days (Table 4). Event days exhibit a distinct new particle (nucleation;
270 3-25 nm) mode which lasts for hours and shows signs of particle growth, while particles during non-
271 event days display a bimodal size distribution with Aitken (25-100 nm) and accumulation (> 100 nm)
272 modes (Dal Maso et al., 2005). Days that did not fulfil either criteria, exhibiting sporadic occurrences
273 of nucleation particles or growth in the Aitken mode, were classified as *undefined*. Finally, if missing
274 data were obtained during the day, the entire day was classified as *missing*. Although consideration is
275 needed when interpreting the short monitoring periods in Leicester and London, the calculated NPF
276 frequencies confirm the existence of new particle formation events in the studied urban environments.
277 The obtained frequencies of days containing NPF events are very similar between LE1M (13%), AD1
278 (16%) and AP1 (17%), while more event days were observed in LO1M (36%). In general, NPF events in
279 the urban atmosphere are less favoured than in the rural atmosphere due to the high preexisting
280 surface area for condensation of non-volatile materials needed for homogeneous nucleation (Dall'Osto
281 et al., 2013). Previous studies in urban environments reported on similar NPF frequencies of 14-19%
282 in Barcelona, Madrid and Brisbane (Brines et al., 2015), 13-20% in Barcelona (Dall'Osto et al., 2013;
283 Pey et al., 2008) and 23% in Hong Kong (Wang et al., 2014), more intense nucleation events are
284 observed in cleaner environments due to the lower pre-existing condensation sinks, with 24% in boreal
285 forests (Dal Maso et al., 2005) and >35% in the Himalayas (Venzac et al., 2008).

286 *Table 4: New particle formation events in the SMPS data obtained from Amsterdam (730 days), Antwerp (730*
287 *days), Leicester (31 days) and London (28 days) based on the classification scheme of Dal Maso et al. (2005).*

	AD1		AP1		LE1M		LO1M	
	# days	*%*	*# days*	*%*	*# days*	*%*	*# days*	*%*
Event	118	16.16	121	16.58	4	12.90	10	35.71
Non-event	56	7.67	104	14.25	5	16.13	0	0.00
Undefined	330	45.21	355	48.63	20	64.52	9	32.14
Missing	226	30.96	150	20.55	2	6.45	9	32.14

288

3.4 Relationship with commonly-monitored pollutants

290 To evaluate potential relationships between UFPs and more commonly monitored atmospheric
291 pollutants, 30 minute and daily-averaged TNC was plotted against PM_{10}, $PM_{2.5}$, NO_2, NO and BC
292 concentrations per site. The TNC was linearly related with BC (*Figure 4*), NO_2 (not shown) and NO (not
293 shown), which confirms vehicle engines as an important source of UFPs at the studied sites.

294 However, at the Amsterdam site, relationships between these typical traffic-related pollutants and
295 TNC were significantly weakened. Therefore, traffic may not be the dominant UFP source at this
296 particular monitoring location. The presence of the low emission zone (Panteliadis et al., 2014) and/or
297 contributions from other UFP sources might explain this lack of correlation between traffic-related
298 pollutants and TNC in Amsterdam.

299
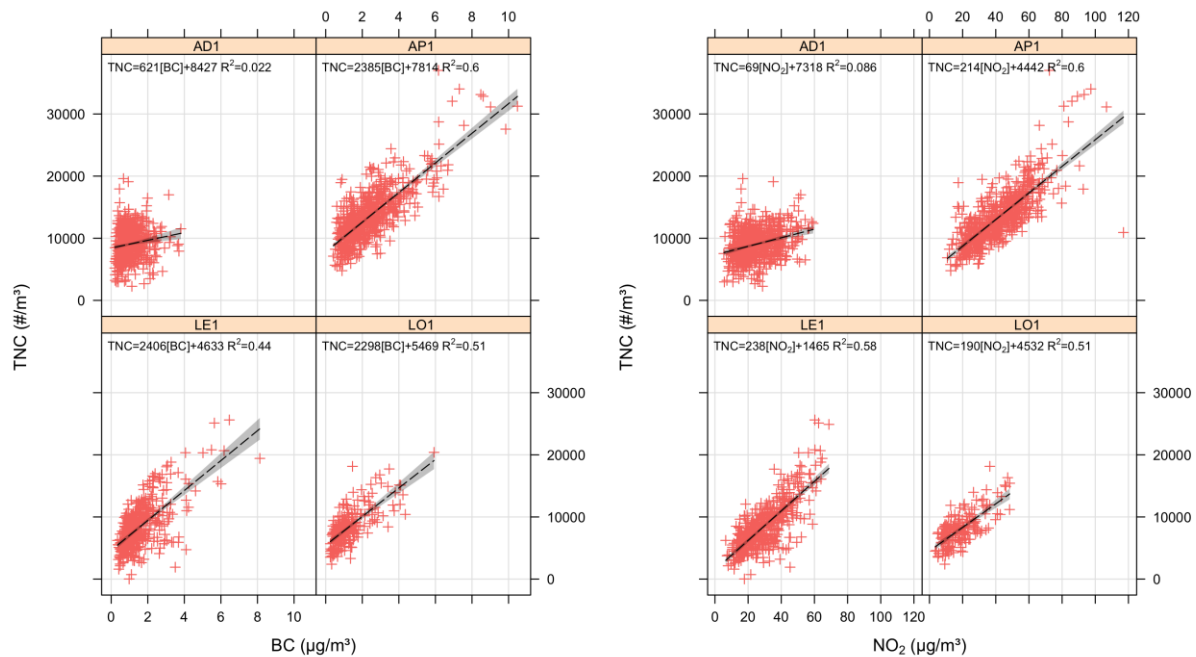
Figure 4: Regression plots of daily-averaged BC (left; µg/m³) and NO₂ (right; µg/m³) versus TNC (#/cm³) at the fixed monitoring sites (AD1, AP1, LE1 and LO1).

The relationships observed between the atmospheric pollutants seemed to exhibit a seasonal variation (not shown). For Antwerp, the strongest correlation obtained between BC and TNC was observed during the winter season ($R^2 = 0.64$). The relationship was weakest during the summer season (June, July, August), which may suggest a higher contribution of non-traffic emitted UFPs, e.g. originating from new particle formation.

3.5 Spatial variation

3.5.1 Inter-urban

The average UFP size distributions within the aggregated particle size classes (*Figure 5*) were generally similar between the considered monitoring locations. Nevertheless, Antwerp seemed to have a slightly higher contribution of 30-50 nm sized particles, while the 10-20 nm size range was proportionally higher in Amsterdam. When normalized for size bin width (dN (dlog Dp)$^{-1}$), highest PNC were obtained near 30-50 nm, except for Amsterdam (20 nm). The TNC was significantly higher in Antwerp, compared to the other monitoring sites (*Figure 5*). This can be explained by considering the proximity (30 m) of the monitoring site to a very busy access road into Antwerp (*Plantin en Moretuslei*). All other monitoring sites are located further away from road traffic (*Figure 1*) and their nearest roads experience lower traffic volumes.

318
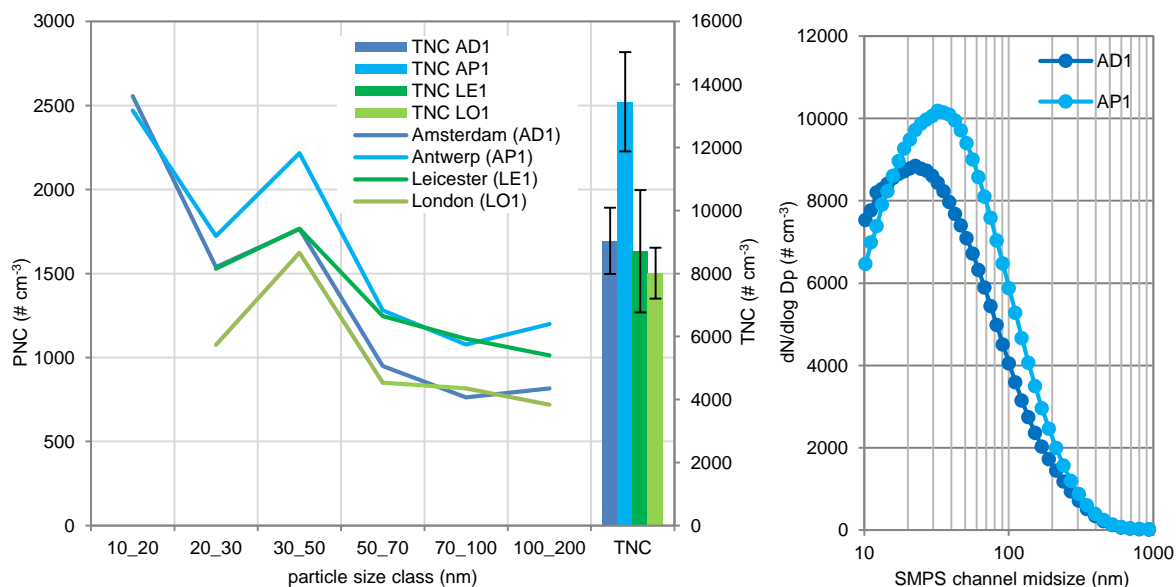
Figure 5: Average size-resolved (PNC; lines) and total (TNC; bars) particle number concentrations for the fixed monitoring locations in Amsterdam, Antwerp, Leicester and London (left) and the full SMPS size distributions with 45 size classes (dN/dlogD$_p$), obtained in Amsterdam and Antwerp (right).

The spatial TNC variation was evaluated by calculating the coefficients of divergence (COD) and Spearman rank correlation coefficients (r_s) between data pairs of the considered monitoring sites (Table 5). Most variation in TNC was observed between the sites in Antwerp and Leicester (COD = 0.37, r_s = 0.30), while the best agreement in TNC was found between Leicester and London (COD = 0.28, r_s = 0.50). Overall, correlations are fairly low (≤ 0.5) indicating that TNC is not related at the regional level of NW Europe and that much of the variation in TNC is, as expected, owing to local factors.

Table 5: Coefficients of determination (COD, left) and Spearman rank correlations (r$_s$, right) of the half-hourly total particle number concentration (TNC) between the respective monitoring sites.

|	COD TNC					Spearman rank (r$_s$) TNC			
	Antwerp	Amsterdam	Leicester	London		Antwerp	Amsterdam	Leicester	London
Antwerp	0.00	0.32	0.37	0.33	Antwerp	1	0.37	0.30	0.38
Amsterdam	0.32	0.00	0.32	0.29	Amsterdam	0.37	1	0.31	0.28
Leicester	0.37	0.32	0.00	0.28	Leicester	0.30	0.31	1	0.50
London	0.33	0.29	0.28	0.00	London	0.38	0.28	0.50	1

330

The COD and correlation coefficients of the individual size classes (Appendix 3) indicate an increased association (smaller COD and larger correlation) was obtained with increasing particle size. As expected, larger particles tend to be more uniform, indicating the regional nature of these aerosols. Long-range transported aerosols comprise mostly of accumulation mode particles, with the major number peak mode around 100-200 nm (Vu et al., 2015). Krudysz et al. (2009) previously found an inverse relationship between particle size and CODs for 13 different monitoring locations within 350 m - 11 km of each other within the city of Los Angeles.

338

339   3.5.2   Intra-urban

340 To explore the spatial TNC variation within the investigated urban environments, a second urban
341 background location (2M) was sampled by means of the mobile monitoring unit in Amsterdam,
342 Antwerp and Leicester (*Table 1*).
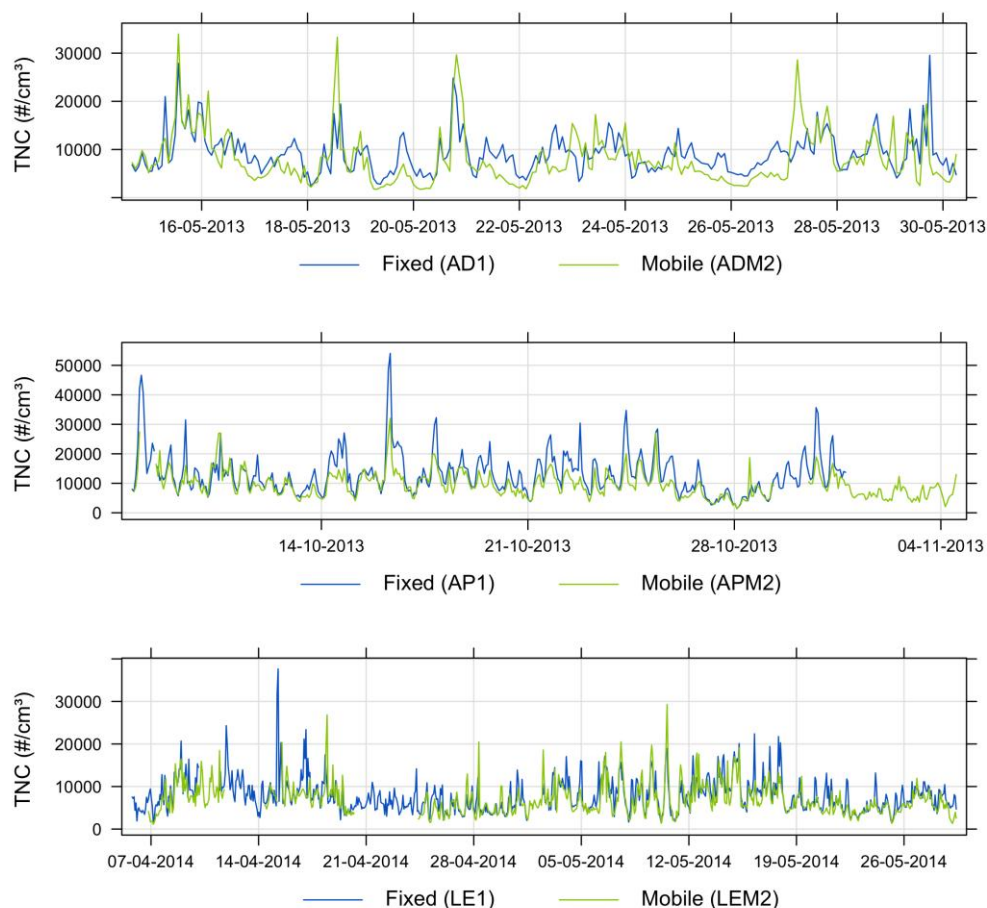
343

344 *Figure 6: Temporal variation of the hourly-averaged total particle number concentration (# cm^{-3}) at the fixed and*
345 *mobile unit locations in Amsterdam (top), Antwerp (middle) and Leicester (bottom).*

346 The hourly-averaged temporal variation plots (*Figure 6*) show that the TNC concentrations at the fixed
347 and mobile monitoring unit locations per city covary in time. In particular for Antwerp and Leicester,
348 the covariance between the two sites seems good, while for Amsterdam some deviations between the
349 sites was observed. The temporal UFP variation seems to consist of two levels. First, there is a (slowly
350 changing) base level which behaves roughly similar in time and magnitude at both paired sites. In
351 particular, this is the case in Antwerp and Leicester, while in Amsterdam there is a small difference of
352 roughly 3000 #/cm^3 between the sites. Looking at the individual particle size classes, it can be seen
353 that this effect is predominantly observed in the 10-20 nm size class, which may be influenced by the
354 different distances of the fixed and mobile sites, respectively, to Schiphol airport. In addition to this
355 base level, part of the fast variation is observed at both sites per city. A clear example was seen in the
356 time series for Antwerp: the peaks at the Stadspark location (AP2M) usually occur simultaneously at
357 Borgerhout (AP1) but have a different magnitude. This was also found at the Leicester sites, and to a
358 lesser extent, at the Amsterdam sites. This could be regarded as an overall urban contribution mostly
359 originating from traffic emissions following a similar behaviour in time but differing in quantity
360 depending on the distance to these emissions source. Apart from these contributions, certain local

361 effects were noted affecting one site but not the other, as can be seen in Amsterdam, which is likely
362 due to a differing influence of a non-traffic source.

363 In addition to the time series plots, coefficients of divergence (COD) and Spearman Rank correlations
364 (r_s) were calculated for the TNC between the fixed and mobile monitoring unit locations in the three
365 cities. As already suggested by the time series plots, the highest association (lowest COD and highest
366 r_s) was obtained in Antwerp (COD = 0.16, r_s = 0.85), followed by Leicester (COD = 0.18, r_s = 0.77) and
367 Amsterdam (COD = 0.25, r_s = 0.59).

368 Nevertheless, the average size distributions at the paired sites per city (*Figure 7*) show large
369 proportional differences in PNC, depending on the particle size class considered. On average, the
370 largest intra-urban variation in TNC was observed in Antwerp (38%), followed by Amsterdam (24%)
371 and Leicester (20%). For Amsterdam, the 10-20 nm PNC was 48% lower at the mobile unit location
372 (AD2M, Nieuwendammerdijk), compared to the fixed monitoring station (AD1, Vondelpark). For
373 Antwerp, the largest difference in size distributions was observed, with up to 49% lower particle
374 numbers for AP2M in the 100-200 nm size range. This is not surprising, as the mobile unit location was
375 within an urban park (*Stadspark*), while the fixed monitoring site was located 30 m from a busy access
376 road (Table 1). In Leicester, the largest difference was observed in the 70-100 nm size range, with 30%
377 lower particle number concentrations at the mobile unit location (LE2M), compared to the fixed site
378 (LE1).
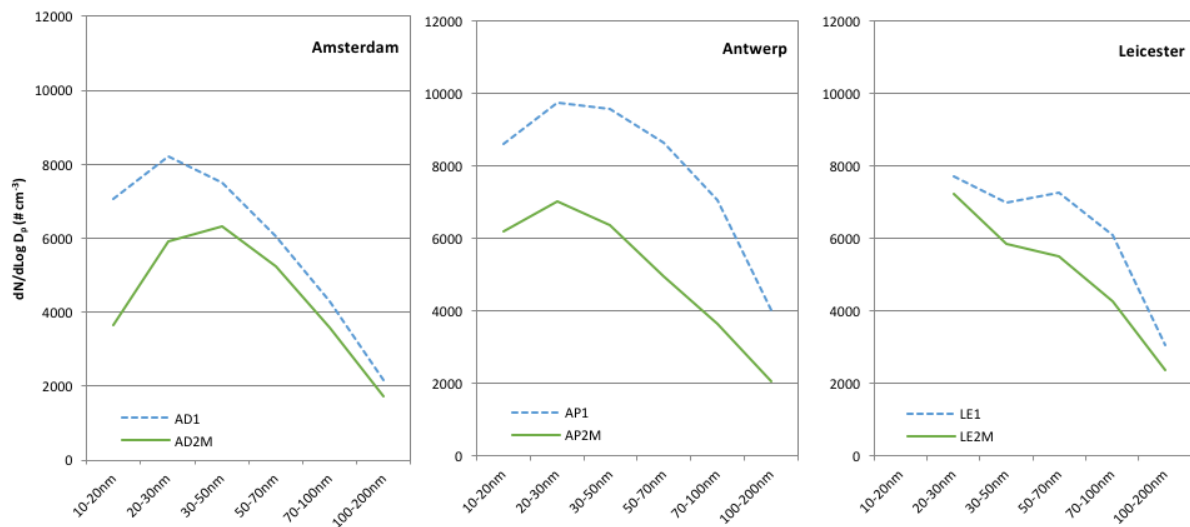
379

380 *Figure 7: Average size-resolved PNC (dN (dlog D_p)$^{-1}$) at the fixed (_1; dashed blue line) and mobile unit (_2M; solid*
381 *green line) locations in Amsterdam (left), Antwerp (middle) and Leicester (right).*

382 Although the UFP number concentrations covaried in time at the monitored locations, considerable
383 proportional differences in size-resolved number concentrations were obtained between the
384 individual intra-urban sites, influenced by their proximity to local UFP sources. This implies that the
385 location of the UFP monitoring station is of primordial importance when evaluating citizen's exposure
386 to UFP in urban environments. In epidemiological studies, UFP data from a single monitoring site are
387 generally used as a measure of population exposure in a wider region. One reason for this is the lack
388 of sufficient data at other sites, which may potentially result in exposure misclassification. While the
389 spatial variation in particle mass concentration is known to be relatively low over an urban region, our
390 results show that this is not the case for particle numbers.

391   3.6 Influence of wind field on measured UFP concentrations

392   All the monitoring sites in this study are classified as urban background stations. In order to assess the
393   influence of local sources on the measured UFP concentrations, the potential effect of the experienced
394   wind field on the total and size-resolved PNC was evaluated. In former studies, wind direction and
395   speed have been shown to be the dominant influencing factors in the spatial variability of PNC (Keuken
396   et al., 2015; Kozawa et al., 2012; von Bismarck-Osten et al., 2013). From the wind roses shown in *Figure*
397   *8*, it is clear that the main wind direction in Amsterdam, Antwerp and London is from the southwest.
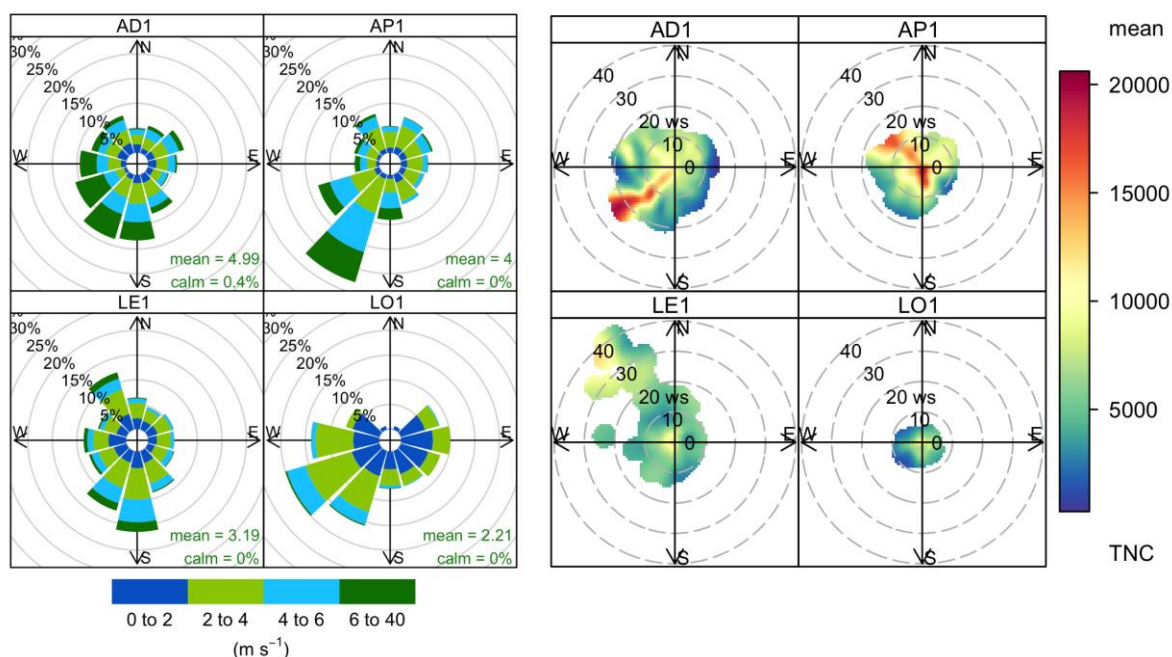
398

399   *Figure 8: Wind roses (left) and polar plots of the average total number concentration (# cm^{-3}, right) with respect*
400   *to the experienced wind direction and speed for the considered monitoring periods at the fixed monitoring sites*
401   *in Amsterdam, Antwerp, Leicester and London.*

402   Polar plots of TNC averaged according to wind direction and wind speed (*Figure 8*, right panel) show
403   clear site-dependent effects. While TNC was relatively independent of wind direction and wind speed
404   in Leicester and London, Amsterdam and Antwerp show significant TNC variation depending on the
405   experienced wind fields. Based on the polar plots, the location of contributing UFP sources can be
406   derived. The polar plot for Antwerp indicated that the site is near a southern-located UFP source,
407   namely the traffic-intensive *Plantin en Moretuslei*. The highest UFP concentations in Antwerp were
408   observed under low wind speeds. At higher wind speeds, UFP emitted by the local traffic will be
409   diluted, resulting in lower UFP concentrations. An additional UFP input can be observed when the wind
410   is blowing from the NW, where streets at the other side of the monitoring site are located, as was also
411   observed in (VMM, 2014). Looking at the individual size classes, the source effect of the *Plantin en*
412   *Moretuslei* is most apparent for the 20-30 and 30-50 nm size classes (not shown). For the Amsterdam
413   site, an average increase in TNC of 38% can be observed under strong SW winds. Looking at the
414   individual size classes, the increase in TNC for SW winds was only observed for the 10-20 and 20-30
415   nm size classes (not shown). This might be attributable to Schiphol airport emissions, in line with
416   Keuken et al. (2015), who recently reported on a marked UFP increase in Amsterdam dominated by
417   10-20 nm sized particles during periods when the wind was blowing from the direction of Schiphol

airport. The TNC increased by a factor of three at a monitoring station (Adamse Bos) located 7 km from Schiphol (Keuken et al., 2015). This study was later confirmed by Bezemer et al. (2015). A study near Los Angeles International airport reported on a comparable 4- to 5-fold increase in particle number concentrations downwind of the airport at 8-10 km (Hudda et al., 2014). Other studies near airports in Zurich (ACI EUROPE, 2012), Copenhagen (Ellerman et al., 2012; Møller et al., 2014), Stockholm (ACI EUROPE, 2012), Santa Monica (Hu et al., 2009) and Los Angeles (Westerdahl et al., 2008; Zhu et al., 2011) confirmed aviation as an important small-sized (< 40 nm) UFP source, predominantly exhibited at the airport and downwind locations. The health-relevance of these airport-related particles is however unclear due to the current lack of toxicological evidence.

Taking into account the location of the Amsterdam site (AD1) at approximately 8 km downwind of Schiphol Airport (Figure 10), the non-traffic-related temporal variation of the 10-20 nm size range which persists throughout the weekends (see 3.3), and no clear relation between TNC and traffic-related pollutants (see 3.2), Schiphol seems to contribute to the urban UFP concentrations in Amsterdam. The TNC, measured at the AD1 site, was observed to increase by 34% when the wind was blowing from Schiphol (205-245°) compared to all other wind directions. As the city centre of Amsterdam is located downwind of Schiphol airport and south-westerly wind directions were experienced for 16% of the total monitoring time (5436 half-hourly values on a total of 34830 half-hourly values were between 205-245°), a significant attribution of Schiphol on citizens' exposure in Amsterdam can be expected. Taking into account the 34% TNC increase and 16% occurrence of 205-245° wind directions, Schiphol airport determined 5.44% of TNC at the Amsterdam monitoring station near Vondelpark (city centre of Amsterdam). Plotting the PNC of the smallest size class (10-20 nm) as a function of wind direction, this directional effect becomes much stronger as the 10-20 nm PNC is almost doubled (99% increase) when wind is blowing from 205-245° (*Figure 9*). Although less clear due to the much shorter monitoring period (2 weeks) and the possible upwind influence of Amsterdam itself, higher 10-20 nm concentrations were obtained as well at the trailer location (AD2M) when the wind was blowing from the SW. Taking into account the 16% occurrence of 205-245° wind directions, Schiphol airport accounted for 16% of the PNC of 10-20 nm particles at the AD1 monitoring site.

For Leicester, a slight increase in TNC was observed for periods in which wind was blowing from the west (NW-SW). Potential contributors might be East Midland airport and Radcliffe Soar power station, which are both located at about 27 km NW of the considered monitoring site. These more distant source locations appear to be reflected in the observed contribution at the monitoring site under high (>20 m s^{-1}) wind speeds. A north-south oriented main road (Welford Road) surrounded by residential areas is situated west of the Leicester site and a green area and Leicester University are situated east of the station. As the temporal variation shows a traffic-related diurnal variation, it can be assumed that the main road is contributing significantly to the measured PNC. The highest contribution in PNC during western wind conditions was observed for the 20-30 nm size class (not shown).

The site in London shows rather homogeneous particle number concentrations independent of the experienced wind fields. No clear effect of London Heathrow airport (± 35 km in western direction) or London city airport (± 8 km north) was observed on the measured UFP concentrations. Based on the wind rose in Figure 9, London experienced negligible (< 1%) northern wind fields, excluding a potential influence of London city airport in our UFP data. Only during strong and eastern wind conditions, an increase in TNC was observed. This might be due to the Port of London, which is located at about 15 km in the eastern direction of the LO1 monitoring site. Previous studies already reported significant UFP contributions from shipping in coastal regions (González et al., 2011; Healy et al., 2009; Querol et al., 2011).

4. Conclusion

This study reports on a 1-2 year-long time series of total and size-resolved UFP number concentrations at four European urban background locations (Amsterdam, Antwerp, Leicester and London), supplemented with additional short-term mobile monitoring unit measurements (2-4 weeks) at an additional urban background location in Amsterdam, Antwerp and Leicester. The obtained time series provide important insights into the spatiotemporal variation of total and size-resolved UFPs in urban environments. While UFP sizing instruments represent feasible additions to air quality monitoring networks, best data coverage (comparable to traditional monitors) requires more maintenance and expertise than for traditional monitors. The co-located mobile monitoring unit provided a valuable addition to the fixed sites for harmonisation and validation purposes.

The fixed monitoring sites show comparable UFP size distributions with similar proportional contributions between the individual particle size classes (100-200 < 70-100 < 50-70 < 20-30 < 30-50 < 10-20 nm). Nevertheless, the size-resolved measurements enabled us to identify different contributing emission sources at different spatial scales. When comparing UFP size distributions between the various sites, better association was obtained between the larger UFP size classes (>50 nm). Larger particles, therefore, seem to be more uniform in space, which confirms the regional nature of these aerosols. Ambient UFP concentrations, in line with BC and NO$_2$, showed clear traffic-related diurnal variation with distinct morning and evening rush hour peaks on week days, but only a clear evening peak during the weekends. Apart from the diurnal traffic-related variation, new particle formation events were observed in all cities for 13-36% of the days. Compared to the other sites, Antwerp experienced significantly higher TNC owing to its proximity to a busy road, confirming road traffic as an important UFP source in urban environments.

For Amsterdam, a clear increase in TNC due to increases in the 10-20 and 20-30 nm PNC was observed during strong SW winds. In combination with the high and continuous 10-20 nm contribution throughout the week and the weaker relationships between UFP and BC/NO$_x$, this suggests an influence of Schiphol airport on UFPs measured at a distance of 8 km in the city centre of Amsterdam. Taking into account the frequency of southwestly wind fields, and the proportional increase of total and 10-20 nm sized particles, Schiphol airport was estimated to potentially contribute up to 5% of TNC and 16% of 10-20 nm particles measured at the Amsterdam site.

The spatial variation of UFPs inside the respective cities was evaluated using simultaneous mobile monitoring unit measurements at additional urban background locations. Although covarying UFP concentrations were observed (r_s = 0.59 to 0.85), the absolute difference in terms of particle numbers have been shown to be significant (up to 38% and 49% for total- and size-resolved particle numbers, respectively). As all monitoring sites are classified as "urban background" locations, the observed differences will likely even increase between more contrasting locations. This implies that the location of the UFP monitoring site is of primordial importance when evaluating citizen's exposure to UFPs in urban environments. Compared to the total number concentration, size-resolved measurements have been shown to offer far more information on the type, origin and transformation processes of atmospheric aerosols. Moreover, by combining both total and size-resolved UFP instruments, instrument anomalies can be detected more easily.

Acknowledgments

Supplementary Material

Appendix 1: Temporal variation of BC (μg m⁻³) for the considered monitoring stations (AD1, AP1, LE1 and LO1)
at three different time scales (monthly, daily and hourly averages). The coloured zone represents the 95%
confidence interval.
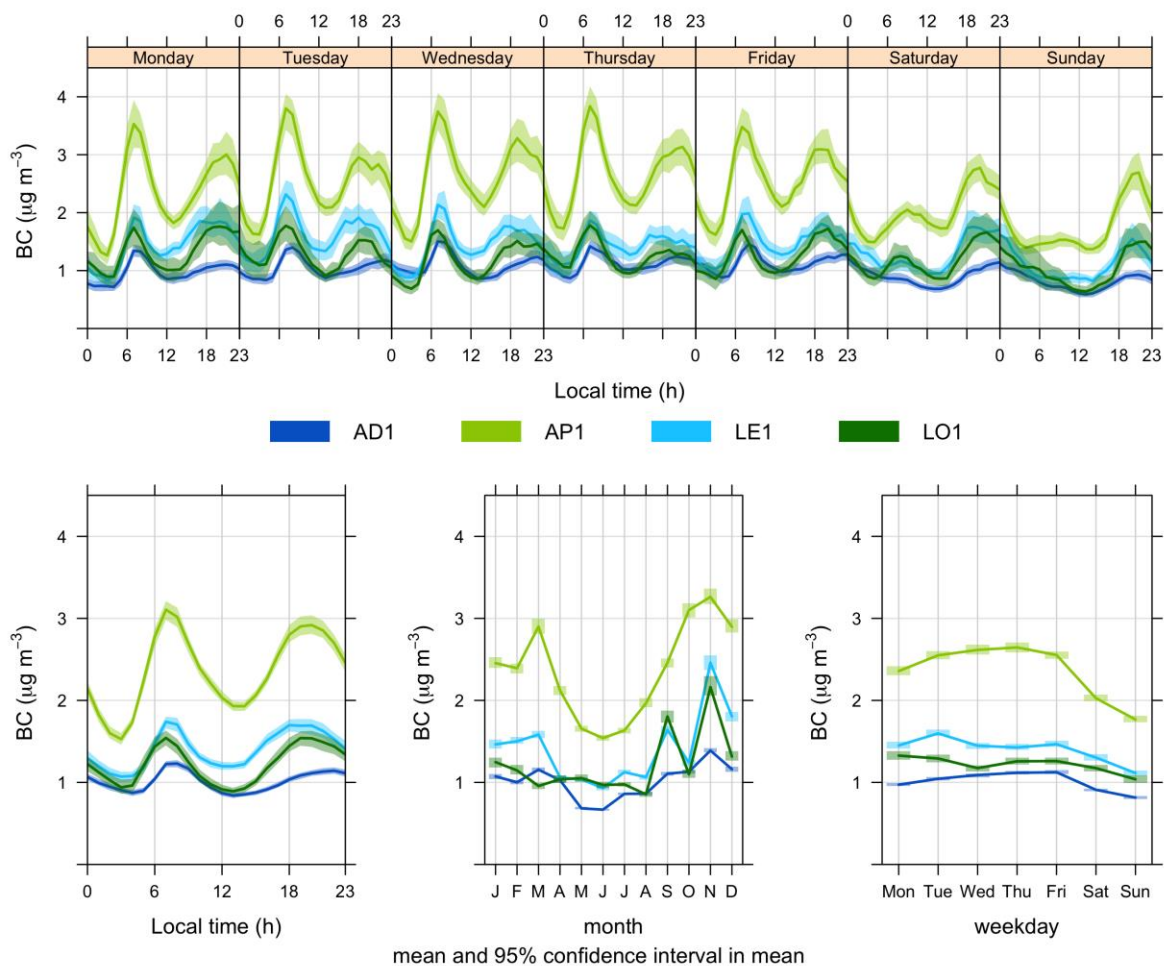
527

528

529

530

531

532

533

534

535

536

Appendix 2: Temporal variation of the size-resolved particle number concentration (# cm^{-3}) obtained at the
Amsterdam (AD1, upper) and Antwerp (AP1, lower) monitoring site within the 10-20 nm, 20-30 nm, 30-50 nm,
50-70 nm, 70-100 nm and 100-200 nm size classes at three different time scales (monthly, daily and hourly
averages).

546 *Appendix 3: Coefficients of determination (COD, left) and Spearman Rank correlations (r_s, right) of the half-*
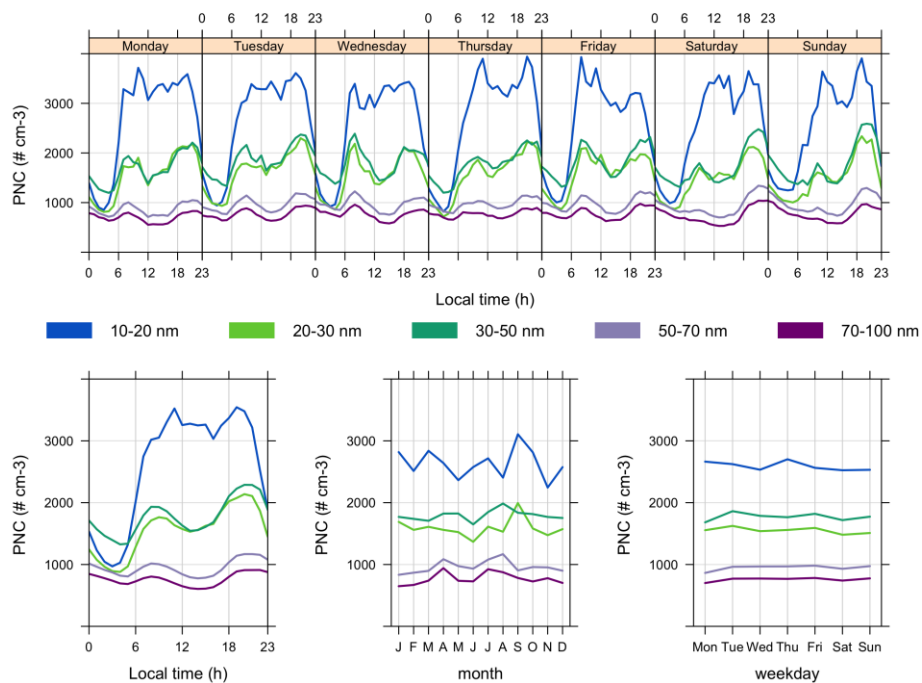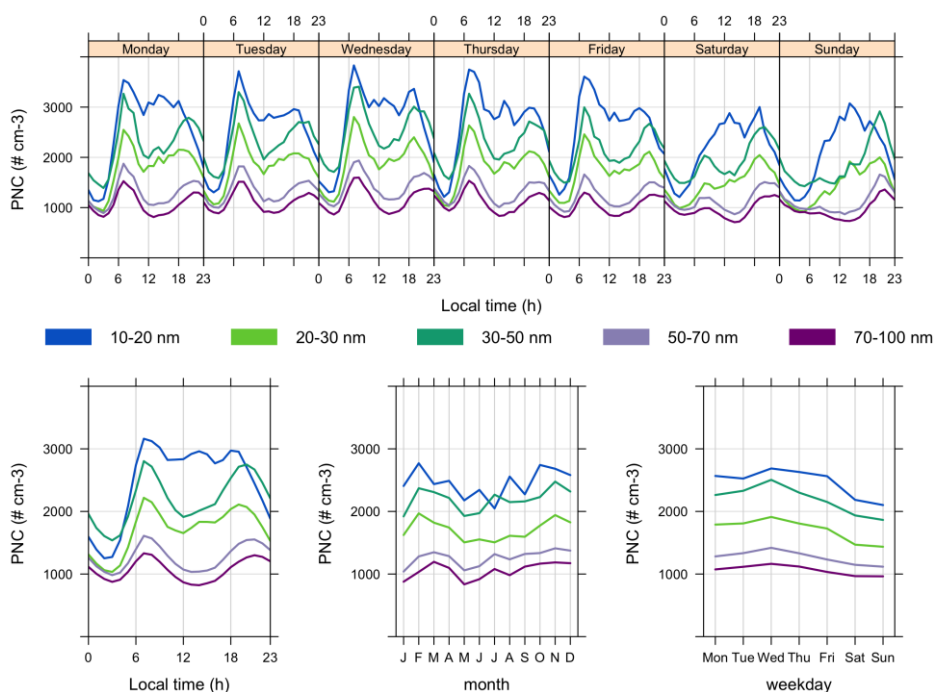547 *hourly size-resolved particle number concentrations between the respective monitoring sites. Only for Antwerp*
548 *and Amsterdam, 10-20 nm size class measurements were available (SMPS).*

COD 10-20 nm

	Antwerp	Amsterdam	Leicester	London
Antwerp	0.00	0.36	NA	NA
Amsterdam	0.36	0.00	NA	NA
Leicester	NA	NA	NA	NA
London	NA	NA	NA	NA

Spearman rank (r_s) 10-20 nm

	Antwerp	Amsterdam	Leicester	London
Antwerp	1.00	0.37	NA	NA
Amsterdam	0.37	1.00	NA	NA
Leicester	NA	NA	NA	NA
London	NA	NA	NA	NA

COD 20-30 nm

	Antwerp	Amsterdam	Leicester	London
Antwerp	0.00	0.33	0.35	0.44
Amsterdam	0.33	0.00	0.36	0.42
Leicester	0.35	0.36	0.00	0.40
London	0.44	0.42	0.40	0.00

Spearman rank (r_s) 20-30 nm

	Antwerp	Amsterdam	Leicester	London
Antwerp	1.00	0.36	0.31	0.11
Amsterdam	0.36	1.00	0.29	0.17
Leicester	0.31	0.29	1.00	0.34
London	0.11	0.17	0.34	1.00

COD 30-50 nm

	Antwerp	Amsterdam	Leicester	London
Antwerp	0.00	0.31	0.35	0.37
Amsterdam	0.31	0.00	0.35	0.35
Leicester	0.35	0.35	0.00	0.32
London	0.37	0.35	0.32	0.00

Spearman rank (r_s) 30-50 nm

	Antwerp	Amsterdam	Leicester	London
Antwerp	1.00	0.38	0.35	0.17
Amsterdam	0.38	1.00	0.25	0.15
Leicester	0.35	0.25	1.00	0.35
London	0.17	0.15	0.35	1.00

COD 50-70 nm

	Antwerp	Amsterdam	Leicester	London
Antwerp	0.00	0.30	0.34	0.39
Amsterdam	0.30	0.00	0.38	0.36
Leicester	0.34	0.38	0.00	0.35
London	0.39	0.36	0.35	0.00

Spearman rank (r_s) 50-70 nm

	Antwerp	Amsterdam	Leicester	London
Antwerp	1.00	0.48	0.39	0.21
Amsterdam	0.48	1.00	0.27	0.18
Leicester	0.39	0.27	1.00	0.38
London	0.21	0.18	0.38	1.00

COD 70-100 nm

	Antwerp	Amsterdam	Leicester	London
Antwerp	0.00	0.32	0.35	0.38
Amsterdam	0.32	0.00	0.41	0.37
Leicester	0.35	0.41	0.00	0.35
London	0.38	0.37	0.35	0.00

Spearman Rank (r_s) 70-100 nm

	Antwerp	Amsterdam	Leicester	London
Antwerp	1.00	0.60	0.39	0.17
Amsterdam	0.60	1.00	0.31	0.18
Leicester	0.39	0.31	1.00	0.36
London	0.17	0.18	0.36	1.00

COD 100-200 nm

	Antwerp	Amsterdam	Leicester	London
Antwerp	0.00	0.32	0.36	0.44
Amsterdam	0.32	0.00	0.38	0.40
Leicester	0.36	0.38	0.00	0.36
London	0.44	0.40	0.36	0.00

Spearman rank (r_s) 100-200 nm

	Antwerp	Amsterdam	Leicester	London
Antwerp	1.00	0.66	0.42	0.27
Amsterdam	0.66	1.00	0.38	0.28
Leicester	0.42	0.38	1.00	0.48
London	0.27	0.28	0.48	1.00

549

550

551 Bibliography

552

553 ACI EUROPE, 2012. Ultrafine Particles at Airports: Discussion and assessment of ultrafine particles (UFP) in
554   aviation and at airports in 2012.

555 Bezemer, A., Wesseling, J., Cassee, F., Fischer, P., Fokkens, P., Houthuijs, D., Jimmink, B., de Leeuw, F., Kos, G.,
556   Weijers, E., Keuken, M., Erbrink, H., 2015. Further exploratory study of ultrafine particulate material
557   around Schiphol. RIVM.

558 Brines, M., Dall'Osto, M., Beddows, D.C.S., Harrison, R.M., Gómez-Moreno, F., Núñez, L., Artíñano, B., Costabile,
559   F., Gobbi, G.P., Salimi, F., Morawska, L., Sioutas, C., Querol, X., 2015. Traffic and nucleation events as
560   main sources of ultrafine particles in high-insolation developed world cities. Atmospheric Chemistry and
561   Physics 15, 5929–5945. doi:10.5194/acp-15-5929-2015

562 Carslaw, D.C., Ropkins, K., 2012. openair — An R package for air quality data analysis. Environmental Modelling
563   & Software 27-28, 52–61. doi:10.1016/j.envsoft.2011.09.008

564 Carslaw, D.C., Ropkins, K., 2015. openair: Open-source tools for the analysis of air pollution data. Natural
565   Environment Research Council, London.

566 Dal Maso, M., Kulmala, M., Riipinen, I., Wagner, R., Hussein, T., Aalto, P.P., Lehtinen, K.E.J., 2005. Formation and
567   growth of fresh atmospheric aerosols: eight years of aerosol size distribution data from SMEAR II,
568   Hyytiälä, Finland.

569 Dall'Osto, M., Querol, X., Alastuey, A., O'Dowd, C., Harrison, R.M., Wenger, J., Gómez-Moreno, F.J., 2013. On the
570   spatial distribution and evolution of ultrafine particles in Barcelona. Atmospheric Chemistry and Physics
571   13, 741–759. doi:10.5194/acp-13-741-2013

572 Donaldson, K., Stone, V., Clouter, A., Renwick, L., MacNee, W., 2001. Ultrafine particles. Occup Environ Med 58,
573   211–6, 199.

574 Ellerman, T., Massling, A., Løfstrøm, P., Winther, M., Nøjgaard, J., Ketzel, M., 2012. Assessment of the air quality
575   at the apron of Copenhagen airport castrup in relation to the working environment. Technical Report
576   from DCE – Danish Centre for Environment and Energy.

577 Frijns, E., Van Jo, L., Aerts, W., Brabers, R., Berghmans, P., 2013. UFP instrument comparison at an urban
578   background location in Antwerp.

579 Goel, A., Kumar, P., 2015. Characterisation of nanoparticle emissions and exposure at traffic intersections
580   through fast–response mobile and sequential measurements. Atmos Environ 107, 374–390.
581   doi:10.1016/j.atmosenv.2015.02.002

582 González, Y., Rodríguez, S., Guerra García, J.C., Trujillo, J.L., García, R., 2011. Ultrafine particles pollution in urban
583   coastal air due to ship emissions. Atmos Environ 45, 4907–4914. doi:10.1016/j.atmosenv.2011.06.002

584 Harrison, R.M., Shi, J.P., Xi, S., Khan, A., Mark, D., Kinnersley, R., Yin, J., 2000. Measurement of number, mass and
585   size distribution of particles in the atmosphere. Philosophical Transactions of the Royal Society A:
586   Mathematical, Physical and Engineering Sciences 358, 2567–2580. doi:10.1098/rsta.2000.0669

587 Healy, R.M., O'Connor, I.P., Hellebust, S., Allanic, A., Sodeau, J.R., Wenger, J.C., 2009. Characterisation of single
588   particles   from   in-port   ship   emissions.   Atmos   Environ   43,   6408–6414.
589   doi:10.1016/j.atmosenv.2009.07.039

590 Hu, S., Fruin, S., Kozawa, K., Mara, S., Winer, A.M., Paulson, S.E., 2009. Aircraft emission impacts in a
591   neighborhood adjacent to a general aviation airport in southern California. Environ Sci Technol 43,
592   8039–8045. doi:10.1021/es900975f

593 Hudda, N., Gould, T., Hartin, K., Larson, T.V., Fruin, S.A., 2014. Emissions from an international airport increase
594   particle number concentrations 4-fold at 10 km downwind. Environ Sci Technol 48, 6628–6635.
595   doi:10.1021/es5001566

596 Joaquin, 2015. Monitoring of ultrafine particles and black carbon. Joint Air Quality Initiative, Work Package 1
597   Action 1 and 3.

598 Kelly, F.J., Fussell, J.C., 2012. Size, source and chemical composition as determinants of toxicity attributable to
599   ambient particulate matter. Atmos Environ 60, 504–526. doi:10.1016/j.atmosenv.2012.06.039

600 Keuken, M.P., Moerman, M., Zandveld, P., Henzing, J.S., Hoek, G., 2015. Total and size-resolved particle number
601   and black carbon concentrations in urban areas near Schiphol airport (the Netherlands). Atmos Environ
602   104, 132–142. doi:10.1016/j.atmosenv.2015.01.015

603 Kozawa, K.H., Winer, A.M., Fruin, S.A., 2012. Ultrafine particle size distributions near freeways: Effects of differing
604   wind directions on exposure. Atmos Environ 63, 250–260. doi:10.1016/j.atmosenv.2012.09.045

605 Krudysz, M., Moore, K., Geller, M., Sioutas, C., Froines, J., 2009. Intra-community spatial variability of particulate
606   matter size distributions in Southern California/Los Angeles. Atmospheric Chemistry and Physics 9,
607   1061–1075. doi:10.5194/acp-9-1061-2009

608 Kulmala, M., Kerminen, V., 2008. On the formation and growth of atmospheric nanoparticles. Atmospheric
609   research 90, 132–150. doi:10.1016/j.atmosres.2008.01.005

610 Kumar, P., Morawska, L., Birmili, W., Paasonen, P., Hu, M., Kulmala, M., Harrison, R.M., Norford, L., Britter, R.,
611   2014. Ultrafine particles in cities. Environ Int 66, 1–10. doi:10.1016/j.envint.2014.01.013

612 Mishra, V.K., Kumar, P., Van Poppel, M., Bleux, N., Frijns, E., Reggente, M., Berghmans, P., Int Panis, L., Samson,
613   R., 2012. Wintertime spatio-temporal variation of ultrafine particles in a Belgian city. Sci Total Environ
614   431, 307–313. doi:10.1016/j.scitotenv.2012.05.054

615 Møller, K.L., Thygesen, L.C., Schipperijn, J., Loft, S., Bonde, J.P., Mikkelsen, S., Brauer, C., 2014. Occupational
616   exposure to ultrafine particles among airport employees--combining personal monitoring and global
617   positioning system. PLoS ONE 9, e106671. doi:10.1371/journal.pone.0106671

618 Panteliadis, P., Strak, M., Hoek, G., Weijers, E., van der Zee, S., Dijkema, M., 2014. Implementation of a low
619   emission zone and evaluation of effects on air quality by long-term monitoring. Atmos Environ 86, 113–
620   119. doi:10.1016/j.atmosenv.2013.12.035

621 Petzold, A., Kramer, H., Schönlinner, M., 2002. Continuous Measurement of Atmospheric Black Carbon Using a
622   Multi-angle Absorption Photometer. Environmental Science and Pollution Research.

623 Pey, J., Rodríguez, S., Querol, X., Alastuey, A., Moreno, T., Putaud, J.P., Van Dingenen, R., 2008. Variations of
624   urban   aerosols   in   the   western   Mediterranean.   Atmos   Environ   42,   9052–9062.
625   doi:10.1016/j.atmosenv.2008.09.049

626 Querol, X., Alastuey, A., Pey, J.P., Viana, M.V., Moreno, T., C. Minguillon, M., Amat, F., Pandolfi, M., Perez, N.,
627   Cusack, M., Reche, C., Dall'Osto, M., Ripoll, A., Karanasiou, A., 2011. Ultrafines in the atmosphere.

628 R Development Core Team, 2015. R: A language and environment for statistical computing. R Foundation for

629   statistical computing, Vienna, Austria.

630   Reche, C., Querol, X., Alastuey, A., Viana, M., Pey, J., Moreno, T., Rodríguez, S., González, Y., Fernández-Camacho,
631   R., de la Rosa, J., Dall'Osto, M., Prévôt, A.S.H., Hueglin, C., Harrison, R.M., Quincey, P., 2011. New
632   considerations for PM, Black Carbon and particle number concentration for air quality monitoring across
633   different European cities. Atmospheric Chemistry and Physics 11, 6207–6227. doi:10.5194/acp-11-6207-
634   2011

635   Venzac, H., Sellegri, K., Laj, P., Villani, P., Bonasoni, P., Marinoni, A., Cristofanelli, P., Calzolari, F., Fuzzi, S.,
636   Decesari, S., Facchini, M.C., Vuillermoz, E., Verza, G.P., 2008. High frequency new particle formation in
637   the Himalayas. Proc Natl Acad Sci U S A 105, 15666–15671. doi:10.1073/pnas.0801355105

638   Viana, M., Rivas, I., Reche, C., Fonseca, A.S., Pérez, N., Querol, X., Alastuey, A., Álvarez-Pedrerol, M., Sunyer, J.,
639   2015. Field comparison of portable and stationary instruments for outdoor urban air exposure
640   assessments. Atmos Environ. doi:10.1016/j.atmosenv.2015.10.076

641   VMM, 2014. Intra-urban variability of ultrafine particles in Antwerp (February and October 2013).

642   Von Bismarck-Osten, C., Birmili, W., Ketzel, M., Massling, A., Petäjä, T., Weber, S., 2013. Characterization of
643   parameters influencing the spatio-temporal variability of urban particle number size distributions in four
644   European cities. Atmos Environ 77, 415–429. doi:10.1016/j.atmosenv.2013.05.029

645   Vu, T.V., Delgado-Saborit, J.M., Harrison, R.M., 2015. Review: Particle number size distributions from seven major
646   sources and implications for source apportionment studies. Atmos Environ 122, 114–132.
647   doi:10.1016/j.atmosenv.2015.09.027

648   Wang, D., Guo, H., Cheung, K., Gan, F., 2014. Observation of nucleation mode particle burst and new particle
649   formation events at an urban site in Hong Kong. Atmos Environ 99, 196–205.
650   doi:10.1016/j.atmosenv.2014.09.074

651   Westerdahl, D., Fruin, S., Fine, P., Sioutas, C., 2008. The Los Angeles International Airport as a source of ultrafine
652   particles and other pollutants to nearby communities. Atmos Environ 42, 3143–3155.
653   doi:10.1016/j.atmosenv.2007.09.006

654   Zhu, Y., Fanning, E., Yu, R.C., Zhang, Q., Froines, J.R., 2011. Aircraft emissions and local air quality impacts from
655   takeoff activities at a large International Airport. Atmos Environ 45, 6526–6533.
656   doi:10.1016/j.atmosenv.2011.08.062

657   Zhu, Y., Hinds, W.C., Kim, S., Shen, S., Sioutas, C., 2002. Study of ultrafine particles near a major highway with
658   heavy-duty diesel traffic. Atmos Environ 36, 4323–4335. doi:10.1016/S1352-2310(02)00354-0

659